Non-destructive profilometry of optical nanofibres; Supporting information

Lars S. Madsen,* Christopher Baker, Halina Rubinsztein-Dunlop, and Warwick P. Bowen

Centre for Engineered Quantum Systems, School of Mathematics and Physics, The University of Queensland, St. Lucia, Brisbane, Queensland 4072, Australia

E-mail: m.lars@uq.edu.au

Methods

The imaging method is implemented in our fibre puller setup without requiring any major additional equipment. The two computer controlled micrometre stages (Newport 561-FH on MFA CC via a ESP 300) which are used to hold and stretch the fibre while tapering are here used to move the sample fibre relative to the probe fibre. The probe fibre is a tapered fibre, glued to an orthogonal fibre clamp that can be brought into contact with the sample fibre with a manual xz-micro-meter stage, see Figure S1. 780 nm light from a Velocity 6312 diode laser is split in two parts with a fibre beamsplitter. One part is measured directly with a Thorlabs PDA10CS-EC photodetector for intensity stabilisation. The other part is sent through the sample fibre and then measured on a identical detector. To minimize back reflection all fibre connections are angle polished (FC/APC) except the output of the sample which is just cleaved. The electronic signals from the detectors are digitalised with a DAQ (NI PCI 6221). The probe is positioned to scatter 40% of the total light when on the waist of the sample. The scattering is adjusted by changing the thickness of the probe fibre at its contact point with the sample fibre through the z-micrometer stage. The 40% is a compromise between high signal to noise ratio and low hysteresis as discussed later. Both sample and probe need to be lightly tensioned to minimise hysteresis.

In the scan data presented for fibre 1 we use

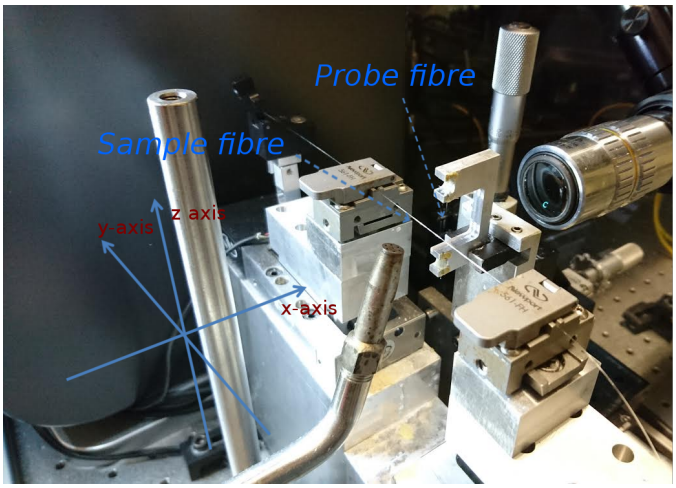

Figure S1: Experimental configuration of the probe and sample fibres. The sample fibre here is not tapered to make it easier to see.

a step size of 0.2 um and 10 ms measurement time. We include a 20 ms pause between moving the probe fibre and measuring the transmission through the sample fibre, in order to allow any vibration caused by the motion of the probe to die out. Each of the transmission data points in figures 2-4a is the average of 1000 samples taken in 10 ms with a 100 kHz sampling rate. In total we obtain an imaging rate of 15 Hz. For fibre 2 we use a stepping size of 1 um and otherwise the same parameters giving a sampling rate of 13 Hz due to the longer step size. During the 302 scans of 600 um length the positioning system measures its own slow drift to a total of 15 um. To have an equal number of measurements at each

*To whom correspondence should be addressed

position we bin the data in 570 bins of 1 um for the statistical analysis, discarding the outer 15 um at each end. The transmission drops 2.1% during the scans. To compensate for this, the 302 scans were normalised to the mean of the 100 right-most points. After this we use the 450 left-most points to determine the relative noise and find a standard deviation of 0.70 nm $\pm$ 0.05 nm.

Scanning electron microscope (JEOL 7100 FEG) imaging of the tensioned ONF is made harder by charging effects as well as electron driven mechanical motion. These effects are alleviated by placing the ONF onto a silicon substrate, and imaging the fibre with low SEM current. The SEM pictures are taken with 30.000 times magnification and 10 kV acceleration voltage. We digitally analyse the SEM images by their brightness, counting pixels which are brighter than twice the average dark noise as fibre. The images have a 960 x 1080 pixels resolution with each pixel corresponding to a scale close to 3 nm x 3 nm. To compare with the scan data we average each image to one data point. The resulting width of the nanofibre is quite sensitive to the choice of threshold value, leading to a systematic radial uncertainty of $\pm$10 nm in the waist region for a threshold value of 1.33 to 2.67 times the average dark noise.

Additional data

The imaging performance with thicker probes is investigated in Supp. Figure S2. We use 4 different positions on the tapered probe fibre providing 4 different probe thicknesses. Figure S2 a) shows that each probe thickness gives a different maximum scattering at the sample waist with the thicker probes scattering more light as expected. The thinnest probe (blue) gives a lower signal-to-noise ratio and we observe artefacts in 3 of the 4 scans with magnitude 0.02 in transmission. The green points correspond to the data presented in the main text in Figure 4. The thick probe (red points) shows a few artefacts; especially we see an undesired jumping near 0.4 mm and a systematic offset between repeated scans on the far right. The offset on the far right is expected to be temporary deformation caused by the drag. Despite these drawbacks the trace displays a very low noise. The

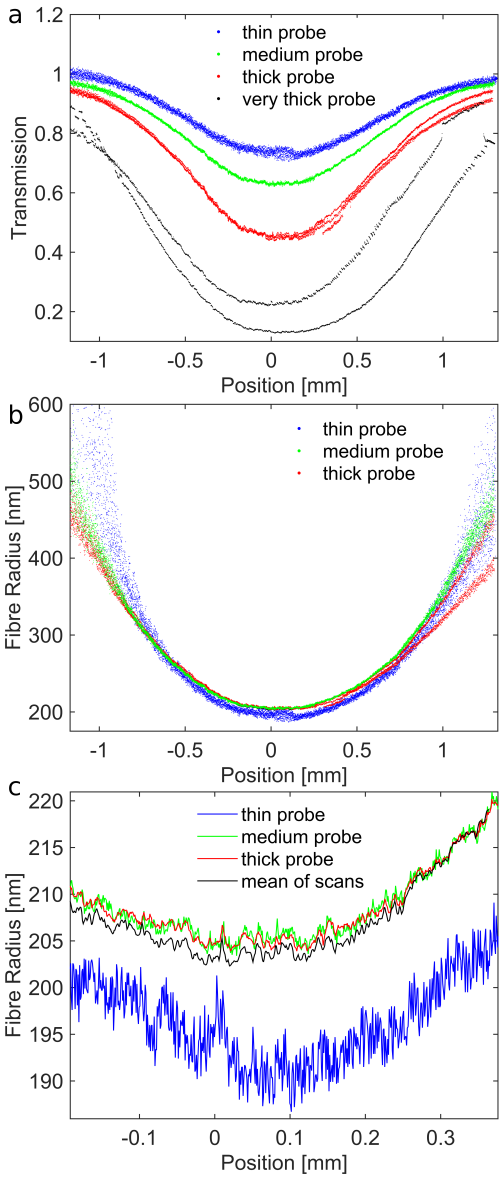

Figure S2: Resolution and hysteresis as function of probe thickness. a) Transmission measurements for 4 probe thicknesses. The data of the medium and thick probes has been compensated for left-right hysteresis of 5um and 6um respectively (green, red). b) Resulting sample fibre radiuses with $\eta = 53\%, 82\%$ and 121% of the outside intensity scattered. c) Zoom-in on central region of b), plotting one scan taken with each probe thickness (thin, medium and large), as well as the mean from the scans in figure 4 b). The data points have been connected to aid the eye.

thickest probe (black) completely deforms the fibre so even though it might have a very low noise it is not suitable for imaging the fibre and so it is only displayed in Figure S2 a). In Figure S2 b)

we have modelled the radius with Eq 1 of the main text, using η of $53\%, 82\%$ and 121% for the thin, medium and thick probes respectively, each found by normalising at the single mode point. The scattering up to $\eta = 121\% > 100\%$ can be explained by coupling between the inside and outside power in the probe region, thereby allowing more than the fraction of power in the evanescent field to be scattered. The data shows that the model still gives the same prediction for the radius in this regime. In Figure S2 c) we zoom in the on the waist region. Here it is clear that the mean of the 302 scans with the medium probe (black trace) and the single pass thick probe (red trace) are in very good agreement showing that our method can reach a resolution of the order of magnitude of 0.1 nm in a single scan.

The polarisation stability of the method and the birefringence of the nanofibre is investigated in Figure S3. The input polarisation of the probe light is controlled with a 3 paddle fibre polarisation rotator. The probe is placed in the middle of the sample and the polarisation is set to either maximum or minimum transmission, resulting in a difference of 10% in transmission. The sample is then imaged for the two settings of the polarisation, see Figure S3a. While changes in sample thickness give correlations in the two traces, birefringence would rotate the maximum and the minimum towards each other giving anti-correlations in their relative separation. To test the methods robustness to input polarisation we derive the radius with the result shown in Figure S3b. Normalization makes sure that the fibres have close to the same thickness in the single mode point. Birefringence and drifts in input polarsation during the measurement would make the two traces drift apart. To magnify the drift we take the difference between the traces shown S3c. The systematic offset comes from the individual calibrations of the single mode point. The maximum difference that the polarisation could cause is 35 nm whereas the observed separation is less than 2 nm. This shows that there is no significant build up of birefringence or drift in input polarization. On the one hand setting the probe to minimum and maximum transmission gives the greatest robustness to such drifts by suppressing the effect of polarisation to first order. On the other hand the sensitivity to birefringence can be maximized by setting the

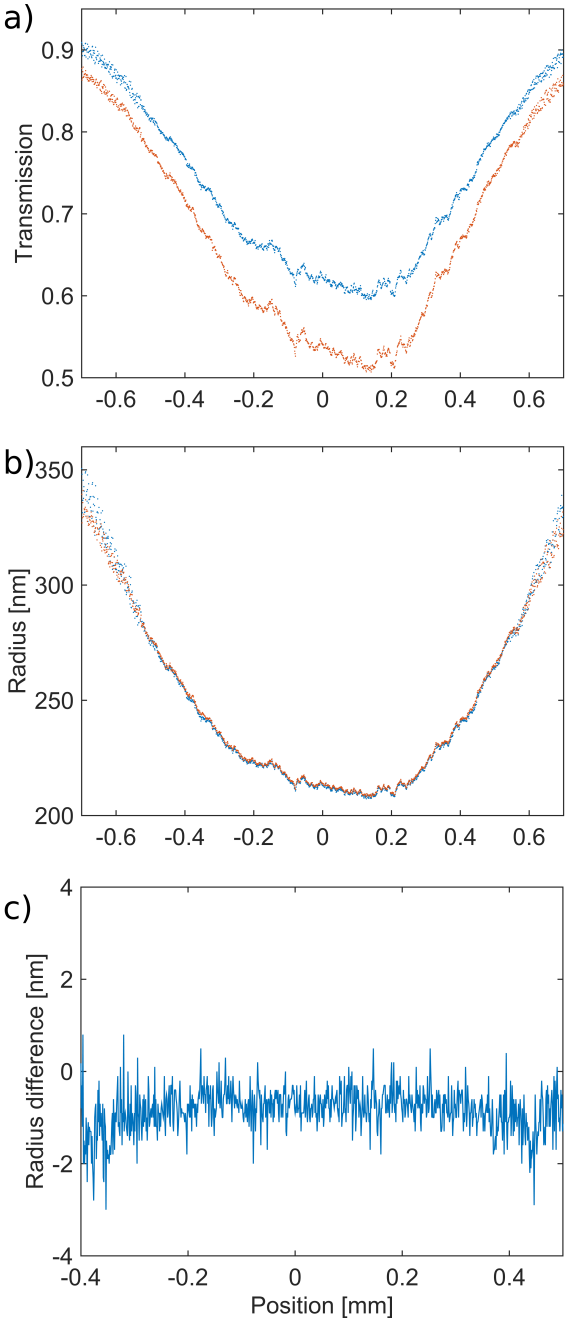

Figure S3: Polarisation data. a) Transmission measurement with the polarisation set to give maximum and minimum transmission on the waist for a single probe thickness. b) Radius calculated from the same data as a) with $\eta = 92\%$ and $\eta = 113\%$ respectively. c) The difference in radius between the traces from b).

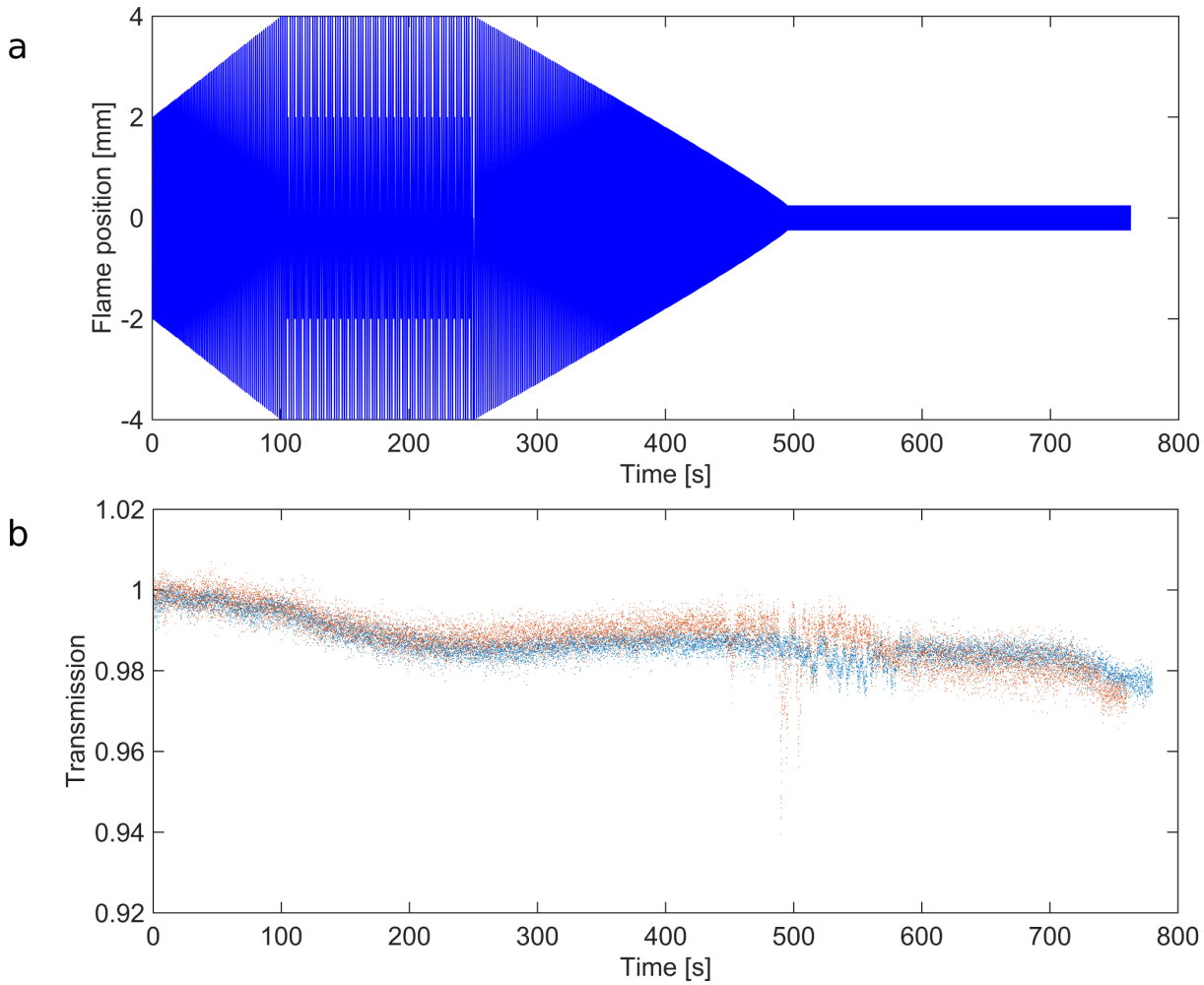

Figure S4: Fabrication data. a) Pattern used to dither the flame along the y-axis while pulling the sample fibres. b) Time traces of the normalised transmission while pulling the sample fibres. Blue points are the first sample fibre and the red points are from the second sample fibre.

polarisation to two orthogonal polarisation states centered between the maximum and minimum.

The fibre puller setup is built around a hydrogen torch on a Newport M-ILS150-ccha stage burning 300 sccm of pure hydrogen (Alicat flowmeter). An optical fibre (Thorlabs 780hp) is stripped and cleaned with acetone. The fibre is held in place by two fibre clamps. The hydrogen torch is dithered back and forth along the y-axis using the pattern shown in Fig. S4 a) while streching the fibre at constant speed. The distance between flame and fibre along the x axis is kept constant in the first 550 seconds, and then moved back 0.2 mm to minimize air turbulence in the final stage of tapering.

While tapering the transmission is measured and recorded with a 20 Hz sampling rate. The power is stabilized as in the main experiment. In Figure S4 b) traces for the two fibres presented in the main text are shown. The onset to multimode operation around 500 seconds is slightly offset and the traces are stopped at slightly different times. This is caused by minor changes in the setup associated with 3 months in between pulling the two fibres and the setup being moved. From the point of view of transmission the final results after the tapering are very similar with close to 98% transmission.

MATLAB Code

The theory needed to model the fibre has been developed by Snyder and Love, Le Kien et al. and in great detail by Vetsch which we follow here.[1–3] We find the propagation constant of the guided mode as function of fibre thickness and use this to

obtain[3] the fraction of power guided inside $\frac{P_{in}(r)}{P_{total}(r)}$ and outside $\frac{P_{out}(r)}{P_{total}(r)}$ of the fibre. Finding the propagation constant is a numerical task, so to efficiently make the conversion between transmission and inferred radius we use a lookup table leaving η as the only fitting parameter. The MATLAB code below generates the table.

```
clear all
close all

%% Parameters
%wavelength
lambda=780*10^-9;
%wavenumber
k_in= 2*pi/lambda;

%refractive indices
%glass (fibre)
n1= 1.46;
% air
n2= 1;
%fibre radii from 175 nm
%to 700 nm in 0.1 nm steps
fiber_radius=175*10^-9:4*10^-10:700*10^-9;
%resolution of probagation constant of fibre,
resolution1=10000;
%propagation constants from n2*k_in to n1*k_in
beta=linspace(1.01*n2*k_in, ...
      n1*k_in*0.99,resolution1);
%%
for fff=1:length(fiber_radius)
%fibre radius
a=fiber_radius(fff);

%% Propagation constant
%Designed for finding the fundamental mode
a_vs_beta=abs(besselj(0,sqrt(k_in^2*n1^2 ...
-beta.^2)'*a)...
./(besselj(1,sqrt(k_in^2*n1^2-beta.^2)'*a)...
.*(sqrt(k_in^2*n1^2-beta.^2)'*a))...
-((n1^2+n2^2)/(2*n1^2)*...
(besselk(0,sqrt(beta.^2-k_in^2*n2^2)'*a)...
+besselk(2,sqrt(beta.^2-k_in^2*n2^2)'*a))...
./(2*(sqrt(beta.^2-k_in^2*n2^2)'*a)...
.*(besselk(1,sqrt(beta.^2-k_in^2*n2^2)'*a)))...
+1./(sqrt(k_in^2*n1^2-beta.^2)'*a).^2 ...
...%-+ for finding other guided modes
-sqrt(((n1^2-n2^2)/(2*n1^2)*...
(besselk(0,sqrt(beta.^2-k_in^2*n2^2)'*a)...
+besselk(2,sqrt(beta.^2-k_in^2*n2^2)'*a))...
./(2*besselk(1,sqrt(beta.^2-k_in^2*n2^2)'*a)...
.*(sqrt(beta.^2-k_in^2*n2^2)'*a))).^2 ...
+(1*beta'/(n1*k_in).*...
(1./(sqrt(beta.^2 -k_in^2*n2^2)'*a).^2 ...
+1./(sqrt(k_in^2*n1^2-beta.^2)'*a).^2)).^2)));
%minimizing the result
% this is for single mode fibres case
if a<n1*0.40*lambda
[~,dummy4]=min(a_vs_beta);
dummy3=0;
%this is needed if there is a higher order mode
else
[~,dummy3]=max(a_vs_beta);
[~,dummy4]=min(a_vs_beta(dummy3:end));
end
beta11=beta(dummy4+dummy3);

%% Fraction of power in and out
h11=sqrt(k_in^2*n1^2-beta11^2);
q11=sqrt(beta11^2-k_in^2*n2^2);
s11=(1/(h11*a)^2+1/(q11*a)^2)...
/((besselj(0,h11*a)-1/(h11*a)...
*besselj(1,h11*a))/(h11*a*besselj(1,h11*a)))...
-0.5*(besselk(0,q11*a)+besselk(2,q11*a))...
/(q11*a*besselk(1,q11*a)));

% fraction P_in/P_total=D_in
%and P_out/P_total=D_out
D_in(fff)=(1-s11)*(1+(1-s11)*beta11^2/h11^2)...
*(besselj(0,h11*a)^2+besselj(1,h11*a)^2)...
+(1+s11)*(1+(1+s11)*beta11^2/h11^2)...
*(besselj(2,h11*a)^2-besselj(1,h11*a)...
*besselj(3,h11*a));
D_out(fff)=besselj(1,h11*a)^2/...
besselk(1,q11*a)^2*((1-s11)...
*(1-(1-s11)*beta11^2/q11^2)...
*(besselk(0,q11*a)^2-besselk(1,q11*a)^2)...
+(1+s11)*(1-(1+s11)*beta11^2/q11^2)...
*(besselk(2,q11*a)^2-besselk(1,q11*a)...
*besselk(3,q11*a)));
end
  %gives the theory curve of inset Fig. 3a
  %in the main text, single mode point at
  %transmission 0.81
eta=1-(1-0.81)/0.19;
figure
```

```
plot(fiber_radius,(D_in+eta*D_out)./(D_in+
    D_out))
xlabel('Fibre radius [m]')
ylabel('Normalised transmission')
```

References

(1) Snyder, A. W.; Love, J. *Optical waveguide theory*; Springer Science & Business Media, 2012.

(2) Le Kien, F.; Liang, J.; Hakuta, K.; Balykin, V. *Optics Communications* **2004**, *242*, 445–455.

(3) Vetsch, E. Optical Interface Based on a Nanofiber Atom- Trap. Ph.D. thesis, Johannes Gutenberg-Universitt, 2010.